ONE POT SYNTHESIS OF Fe_3O_4/MWCNT NANO-COMPOSITE USING NANOMATERIAL SYNTHESIZER

B.Keerthi Priya[1], T.Yasaswi[2], D.V.Rama Koti Reddy[3]

Article History: Received: 21.09.2022 **Revised:** 07.11.2022 **Accepted:** 22.12.2022

Abstract

Iron oxide nanoparticles have attracted considerable interest in various applications owing to their unique properties like their extraordinary magnetic properties, surface area to volume ratio, easy separation and larger surface area. multi-walled carbon nanotubes(MWCNTs) have been investigated considerably, as they have high aspect ratio and good thermal, mechanical, optical, and electrical capabilities. The conjugation between Fe_3O_4 nanoparticles and MWCNT has been found to have enhanced properties. This composite has been found to have multiple applications in biomedical, electronics, etc. In this work, we have used NANOCORPS™ VX100 Nanomaterial Synthesizer for the synthesis of Fe_3O_4 NP/MWCNT nano-composite. The material was characterized and was found to be successfully synthesized.

Keywords: conjugates, iron oxide nanoparticles, carbon nanotubes, nanomaterials synthesis

[1]Department of ECE, Gayatri Vidya Parishad College of Engineering(A),
[2,3]Department of Instrument Technology, Andhra University

DOI: 10.31838/ecb/2022.11.12.144

1. Introduction

Carbon nanotubes (CNTs) are of significant attention in a variety of disciplines owing to its desirable chemical and physical characteristics. CNTs can either be single-walled carbon nanotubes(SWCNTs), multi-walled carbon nanotubes(MWCNTs), nano diamonds (NDs), graphene or fullerene [1]. Due to the Sp^2 bonds between the carbon atoms, MWCNT have a greater tensile strength even as compared to steel [2]. The atomic structure in a MWCNT greatly reduces the collision between conduction, and the robust bonds between carbon atoms permit smooth tolerance of large amounts of electrical current [2]. Due to the hollow structure of MWCNTs, the space inside can be used to encapsulate metal NPs (like iron oxide NPs) which can enhance their magnetic properties. Iron oxide NPs have diameters between 1-100nm, and the two forms of iron oxide NPs are maghemite and its reduced version magnetite [3]. MWCNTs-iron oxide NP conjugates have fascinated a lot of interest due to their extensive use in many fields and its super magnetic properties.

Conjugating iron oxide NPs with nano organic molecules like MWCNTs enhance the repulsive forces on NPs, balancing out the van der Waals and magnetic forces. [4]. Furthermore, conjugating the iron oxide-NPs with MWCNTs offers a promising application in many fields, and thus has been extensively examined due to the conjugate's unique chemical and physical properties. Bare iron oxide NPs (specifically magnetite) is easily oxidised upon contact to air, because they render large amounts of surface energies due to their high surface area-volume ratio [4], and bare MWCNTs do not contain any magnetic properties that limits its use for biomedical applications [5]. Thus, conjugation of MWCNT-iron oxide NPs brings about synergistic effects by combining thermal, optical, and chemical properties of both MWCNT and iron oxide NPs that facilitates in functionalization and stabilization of the nano-system [1, 4].

Most research has been aimed towards developing efficient strategies for the preparation of such conjugates in order to get extremely stable and efficient carbon nanotubes. One commonly used method is *filling process*, which is one of the most facile approaches of fabricating carbon nanotubes [5]. This method is carried out by first filling the CNT pores with Ferro fluid, After that, the precursor of the magnetic species is filled and the precursor is reduced. [6]. In one study, *Bio et al.* fabricated CNTs by feeding Fe NPs into its pores, and subsequently minimizing the metal compounds to form magnetic metals [7]. Advantages of the filling procedure are that the operation is cost efficient, the raw materials are easy to find and the procedure is extremely convenient to perform [5]. However, this process renders a weak reproducibility because the lack of control over the mass ratio of carbon and magnetic precursor. which consequents in the pore getting blocked. Another method used to synthesize conjugates of metal oxides such as Fe_3O_4 and MWCNT is the *sol-gel process* [5]. In this process, hydrolysis and condensation of the precursor is key to this method, and factors such as temperature, pH, and precursor concentration are the most important that governs the ultimate shape, properties, size and quality of the conjugates [8]. *Modugno et al.* synthesized iron oxide-MWCNT nano system using the sol gel method [1]. In their approach, MWCNT was initially stimulated by carboxylic acid groups, following a sol-gel procedure wherein Fe_3O_4 were bonded to the surface of MWCNTs as they were getting simultaneously synthesized [1]. The cost-effectiveness of the sol-gel technique is its main advantage and operates at low temperatures averting the oxidation of precursors is another advantage. On the other hand, a major limitation of this process is that there is a relatively high chance of the product getting contaminated [5].

Chemical Vapor Deposition is a popular synthesis approach in which the process is carried out in a reactive gas compartment [5]. The compartment is filled with gases that have deposition material and coatings that are applied to the substrate [9]. In a report, *Tian et al*. synthesized CNTs filled with iron by the "floating catalyst CVD method" wherein ferrocene was used as an iron source as well as a catalyst precursor [10]. The main advantage of this technique is that the CNT structure is highly controlled, however, the method is expensive and requires high energy procedures [5]. Another well-known procedure is the *Self-assembly* method in which a spontaneous organized structure is formed or "self-assembled" from a haphazard system of components already existing in the system [5]. In this regard, *Zhang et al.* used this approach for the preparation of CNT in a two-step method in which they first obtained hydrophilic CNTs using an oxidizing agent, followed by assembling of iron oxide NPs on CNTs surface [11]. The primary benefit of the self-assembly approach is that it allows good control over MCNTs characteristics, however, the major disadvantage of this approach is the heterogeneity of the product [5].

There are numerous applications of the MWCNT-iron oxide NPs conjugates, of which drug delivery is one of the most prominent. CNTs like MWCNTs are widely used in drug carrier applications because of its exclusive spectroscopic characteristics, as well as their ease of doping with agents that further facilitates their functionality [5]. Conjugation of MWCNTs with magnetic NPs such as iron oxide NPs greatly enhances its potential as a nano-vector as a drug delivery system [12]. CNTs have also extensively been used in gene delivery systems owing to their biocompatibility and non-toxicity and there are one of the most important techniques that can be employed to enhance the efficiency to deliver the exogenous DNA in the target cells is conjugating the MWCNT with iron oxide NPs [5] can facilitate direct delivery of DNA into the nucleus. Another interesting application of these MWCNT-iron oxide NPs conjugate is in hyperthermia [13].

These conjugates are also of great use in theranostic applications such as to detect rare-tumour looking cells [5]. These conjugates penetrate cells without causing damage which renders them useful for the function. In this regards, *Shen et al.* conjugated MWCNTs with iron oxide and non-covalently functionalised with PL-PEG [14]. Other potential application explored for MWCNT-iron oxide conjugate is in their numerous fields of industry. Few examples are using it as a contaminant absorbent (for heavy metal or organic compounds), electrochemical sensors, and magnetic storage medium. *Chen et al.* constructed MWCNT/iron oxide magnetic nanocomposites in order to absorb Nickel and Strontium ions from wastewater [15]. Table1 lists the different routes for synthesis of Fe_3O_4 and MWCNT conjugate along with their merits and demerits.

Table 1. Merits and Demerits of each of the Synthetic methods.

Method	**Merits**	**Demerits**	**Ref.**
Chemical co-precipitation	Simple and effective method.	Large size distribution.	[16]
Hydrothermal, Phase transformation method	Simple and facile method, Ferromagnetic property is kept intact in the synthetic method	Calcination at high temperature is required.	[17]

In situ thermal decomposition method	Size can be controlled.	Magnetic properties is influenced by the reaction conditions.	[18]
Chemical reduction method	Size is controlled, provides active sites of attachment of Fe_3O_4.	May result in agglomeration.	[19]
Green synthesis	The reducing agents or solvents are not used, highly time saving and cost saving.	Agglomeration may be directly proportional to the concentration of the metal precursor used for the reaction.	[20]
Solvo-thermal method	Size & distribution of NPs can be changed depending on concentration.	The presence of water affected the crystal structure of Fe_3O_4 and dispersion on surface of MWCNT	[21]
Microwave assisted method	Fast method, binding efficiency is high, water dispersible particles with superparamagnetic properties.	Cannot be scaled up.	[22]
Spontaneous redox reaction	Effortless method, presence of high defects on the surface of MWNT is favorable for redox reaction and for catalytic application.	The presence of high defects cannot be used for other applications.	[23]
One pot hydrothermal method	Uniform morphology of Fe_3O_4 nanoparticles and wrapping of Fe_3O_4 on MWNT surface, electrical and magnetic properties of MWNT and Fe_3O_4 nanoparticles are retained.	High temperature for calcination is necessary	[24]
Pulsed laser	Avoids harsh chemicals. Reduces processing time	The pulsed laser power may disrupt or break the MWNT structures	[25]
CVD	The nanoparticle dispersion on the MWNT is homogeneous.	Noticed aggregation of nanoparticles according to the concentration of precursors used	[26]
Electrochemical Synthesis	Cost-effective, easily available, high degree of control over other methods, high purity of the product	Determination of the reaction mechanism needs more studies to achieve a full understanding of the process.	This work

In our current work, we have synthesized Fe_3O_4 and MWNT nano-conjugate using the nanomaterial synthesizer manufactured by NANOCORPS^{TM} VX100. We have also synthesized iron oxide nanoparticles (Fe_3O_4) using this instrument. We have

characterized the synthesized Fe_3O_4 nanoparticles and the Fe_3O_4 – MWNT nano-conjugate using XRD, TEM and Raman spectroscopy.

2. Materials And Methods

2.1 Synthesis of Iron oxide nanoparticles (Fe_3O_4)

For synthesis of Fe_3O_4 NPs, NANOCORPS^{TM} VX100 Nanomaterial Synthesizer was used. The iron electrodes were spaced 4 cm apart and fixed. 2M sodium chloride was added in 200 mL double distilled de-ionized water for preparation of electrolyte. 3V DC voltage was given to the electrochemical cell under constant magnetic stirring. After 5 minutes, formation of gas bubbles was observed followed by change in colour of the solution. The whole experiment was carried out at 70°C. The black precipitate obtained was then ultra-sonicated for 30 minutes. The solution was then kept on magnetic stirring overnight. Following that, the material was washed and purified using ultracentrifugation multiple times. The sample was stored at room temperature.

2.2 Synthesis of Fe_3O_4 and MWNT conjugate

For the synthesis of the Fe_3O_4 and MWNT conjugate nanocomposite, NANOCORPS^{TM} VX100 Nanomaterial Synthesizer was used. 2M sodium chloride was added in 200 mL double distilled de-ionized water for the preparation of electrolyte. The electrolyte solution was then sonicated for 3 hours at 37 ° c with 200 mg of MWNT. Iron electrodes were spaced 4 cm apart and fixed. The electrochemical run was performed at 3V DC voltage under constant magnetic stirring. The development of gas bubbles was instantly noticed. The electrolytic solution changed colour to an opaque black precipitate after a few minutes of operation. The experiment lasted 5 minutes at a temperature of 70 degrees Celsius. The residue obtained after the experiment was ultrasonicated for fifteen minutes. In addition, the solution was kept separate from the rest of the batch for overnight stirring. The following day, the sample was washed and purified using ultracentrifugation numerous times to get a pure stock solution in powder form.

2.3 Characterizations/Instruments

A Jeol 2100F microscope was used to conduct transmission electron microscopy (TEM) on all of the sample. XRD carried out using PANalytical X'Pert Pro X-ray diffractometer. Energy-dispersive X-ray study was carried out using EDX integrated system with a Zeiss EVO 40 Scanning electron microscope. Magnetic study was done with the Physical property measurement system (PPMS) from Cryogenics limited. WITec Denmark's combined confocal Raman AFM system was used for Raman spectroscopy.

3. Results And Discussion

3.1 Morphology characterization of Fe_3O_4

Synthesized Fe_3O_4 nanoparticles surface morphology analysed using TEM. TEM image of Fe_3O_4 is shown in Figure 1(a). Average particles size was in the range of 60-80 nm. Figure 1(b) shows the HRTEM image of Fe_3O_4 NPs.d-spacing was 0.257 nm [27].

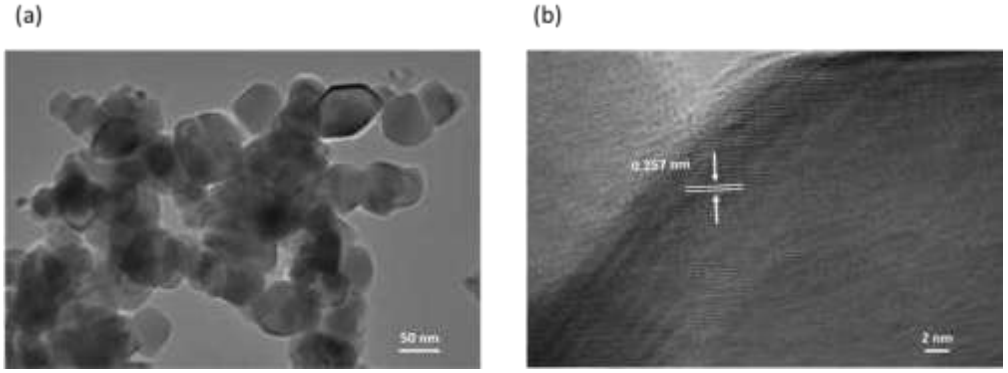

Figure 1. TEM images of Fe_3O_4 NPs ; (a) TEM image, and (b) HRTEM image.

3.2 Structural characterization of Fe_3O_4 nanoparticles

Structural characterization of synthesized Fe_3O_4 NPs was carried out using XRD and selected area electron diffraction (SAED). The X-ray diffraction graph of nanoparticles is shown in Figure 2(a). The major peaks of Fe_3O_4 nanoparticles are present in the graph. The planes signifying these peaks are (220), (311), (400), (422), (511), (440), and (533) [28]. The SAED pattern using TEM was carried out and is shown In Figure 2(b). The planes obtained from the XRD graph can also be seen in the SAED pattern. This pattern typically signifies to the cubic crystal structure of Fe_3O_4 nanoparticles [29, 30].

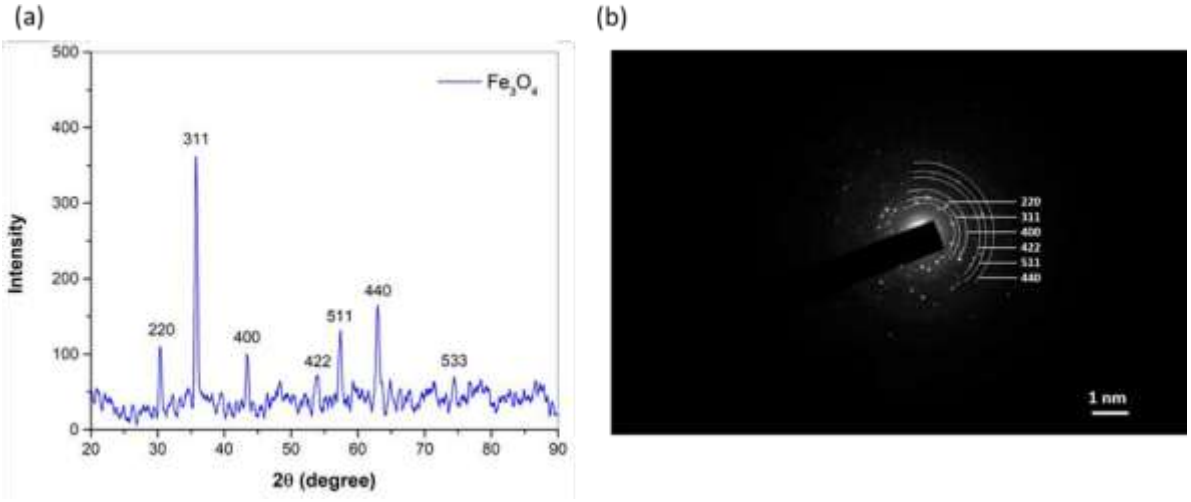

Figure 2. Structural characterizations of Fe_3O_4 nanoparticles; (a) X-ray diffraction graph, and (b) SAED pattern using TEM.

3.3 Morphology characterisation of multi-walled carbon nanotubes

Surface morphology of MWNT was analyzed using TEM. The TEM image of multi-walled carbon nanotubes (MWNT) is shown in Figure 3(a). The average diameter was found to be in the range of 20-25 nm. HRTEM image of the multi-walled carbon nanotubes (MWNT) is shown in Figure 3(b). The d-spacing was calculated to be 0.35 nm [31].

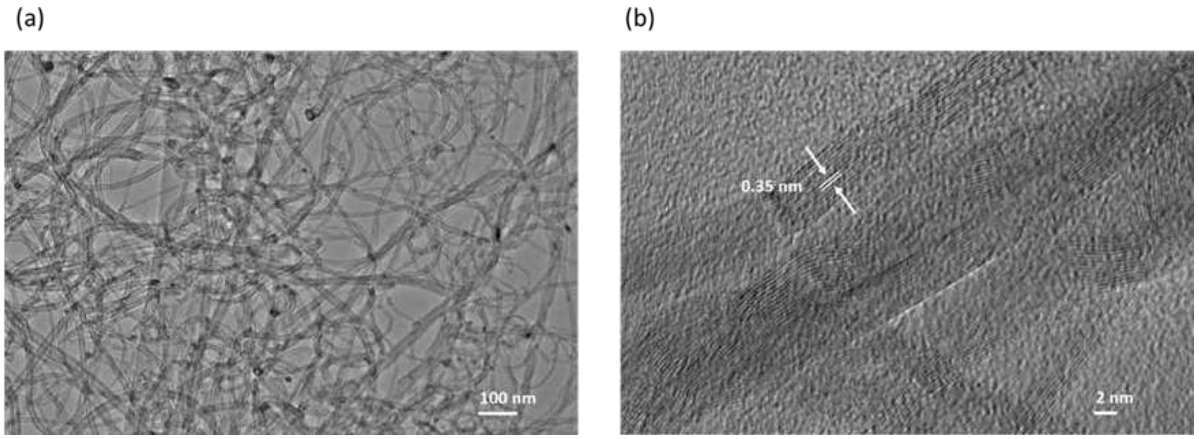

Figure 3. (a) TEM image of MWNT, and (b) HRTEM image of MWNT.

3.4 Vibrational characterisation of MWNTs

Molecular vibrational study of MWNTs was carried using Raman spectroscopy. The Raman spectra show a disorder-induced D band peak at 1343 cm^{-1}, and G band peak at 1576 cm^{-1}. These bands are typical to the presence of MWNT. The peak of the 2D band at 2690 cm^{-1} and a weak G+D peak is also present in the sample [32, 33]. Figure 4 shows the spectrum.

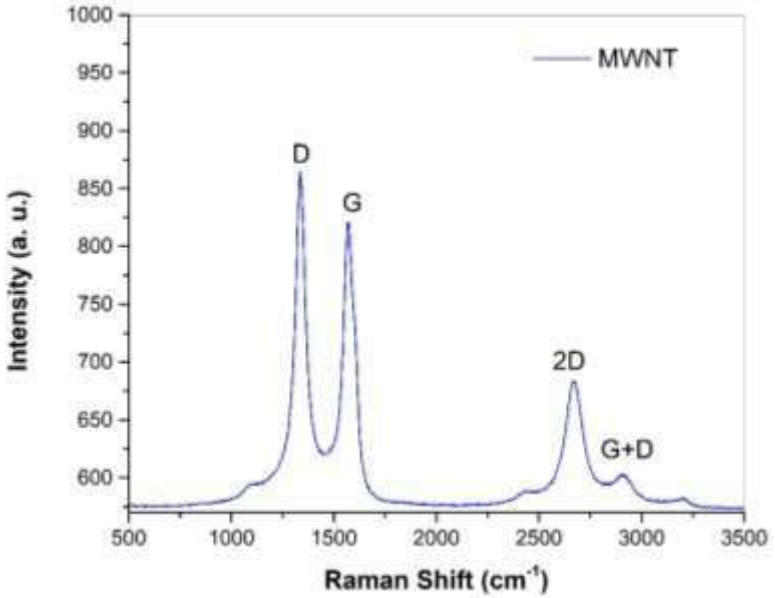

Figure 4. Raman spectra of multi-walled carbon nanotubes (MWNT).

3.5 Morphology characterization of Fe_3O_4 – MWNT nano-conjugate

Surface morphology of the synthesized Fe_3O_4 and MWNT conjugate was analyzed using TEM. The TEM image of Fe_3O_4 nanoparticles and MWNT conjugate is shown in Figure 5. The average particles size of Fe_3O_4 nanoparticles was calculated and was found to be in the range of 80-100 nm. It can be observed from Figure 5 that successful conjugation between Fe_3O_4 and MWNT was achieved through the electrochemical method.

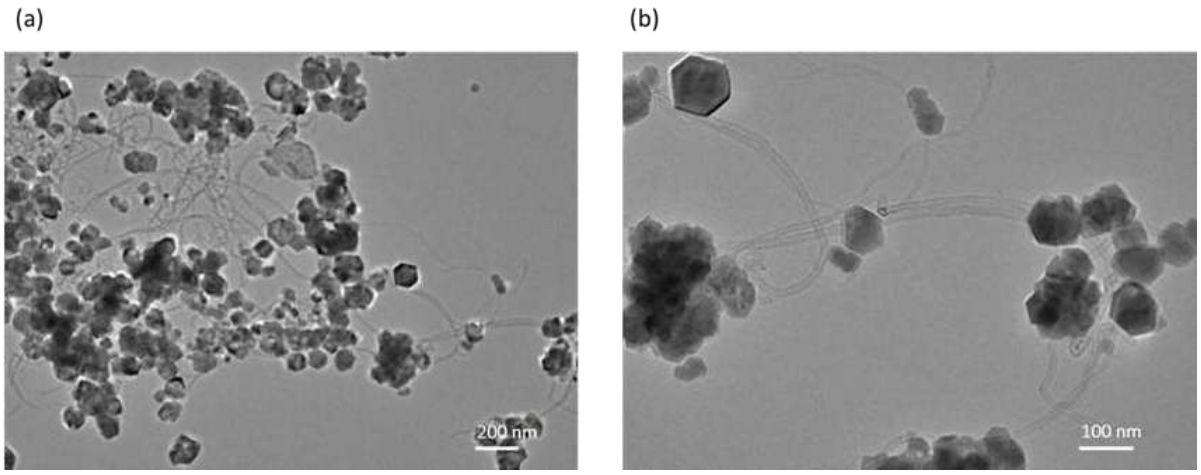

Figure 5. Transmission electron microscopy (TEM) images of Fe_3O_4-MWNT nano-conjugate at (a) 200 nm, and (b) 100 nm scale.

3.6 Vibrational characterization of Fe_3O_4 – MWNT nano-conjugate

The molecular vibrational study for Fe_3O_4 NPs and MWNT was carried using Raman spectroscopy. The Raman spectra show peaks corresponding to both MWNT and Fe_3O_4 nanoparticles. The disorder-induced D band at 1343 cm^{-1} and G band at 1576 cm^{-1} are present which signifies to presence of MWNT in the sample. The peak of 2D band at 2690 cm^{-1} also a weak G+D peak is also present in the sample [32, 33]. The peaks corresponding to Fe_3O_4 nanoparticles are also present at 215, 276, 398, and 654 cm^{-1} [34]. The spectrum is shown in Figure 6 and signifies the successful synthesis of Fe_3O_4 nanoparticles and MWNT.

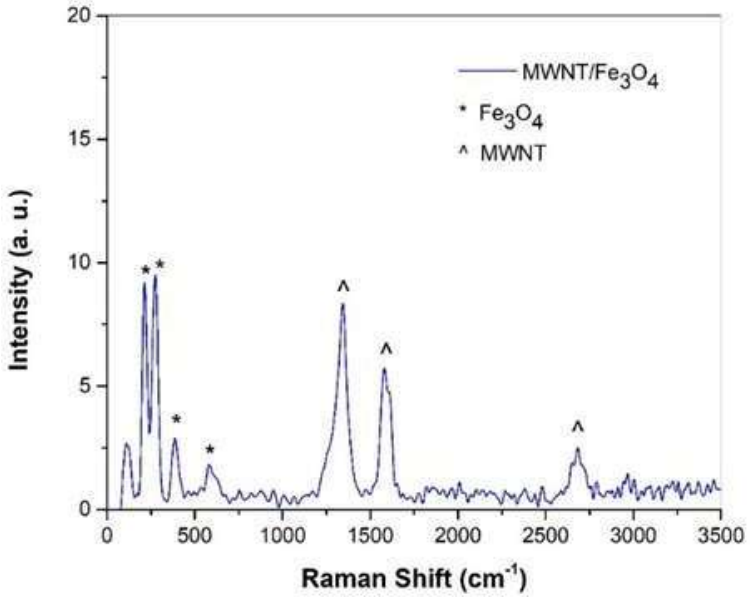

Figure 6. Raman spectra for Fe_3O_4 nanoparticles and MWNT.

3.7 Magnetic and Electrochemical impedance spectroscopy characterization of Fe_3O_4 – MWNT nano-conjugate

The synthesized nanoconjugate of MWNT and Fe_3O_4 was characterized using VSM to study magnetic properties. VSM graph for the MWNT-Fe_3O_4 nanoconjugate is shown

in Figure 7. The hysteresis loop is the curve plotted between the external magnetic field and magnetization (emu/g) of nanoconjugate sample. Hysteresis loop was plotted to study the magnetic property of the MWNT-Fe_3O_4 nanoconjugate. We can observe from the hysteresis loop that the synthesized nanoconjugate between MWNT and Fe_3O_4 nanoparticles exhibit ferromagnetic behaviour. The magnetization saturation value for the synthesized MWNT–Fe_3O_4 nanoconjugate was calculated to be 65.2 emu/g. The magnetization saturation in the case of Fe_3O_4 nanoparticles was achieved at 81.6 emu/g which is higher compared to the magnetization saturation value for MWNT-Fe_3O_4 nanoconjugate. The presence of MWNT in the sample causes a magnetic dead layer. Also, it reduces the amount of Fe_3O_4 nanoparticles in conjugate sample thereby, leading to lower value of magnetic saturation in the case of MWNT-Fe_3O_4 nanoconjugate [35].

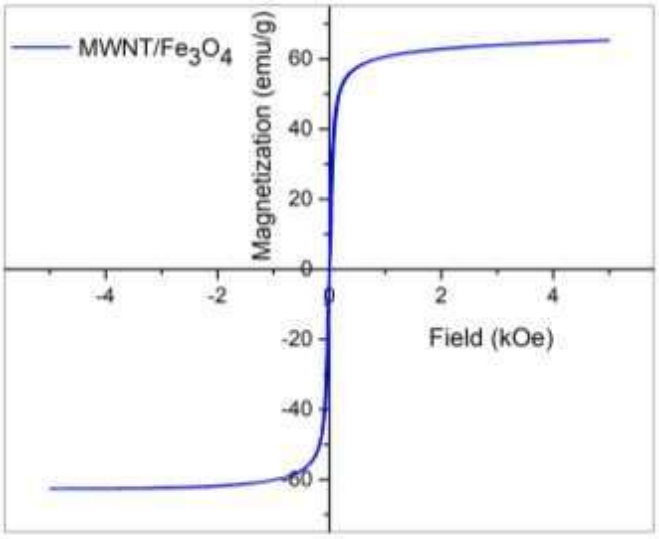

Figure 7: Vibrating sample magnetometer (VSM) graph for Fe_3O_4 and MWNT nanoconjugate.

The electrochemical impedance spectroscopy was carried out to study overall impedance of the system. The spectroscopy was done to evaluate the nyquist response i.e. the plot between the real component (Z') and imaginary component (-Z'') of the impedance. Nyquist plot for the Fe_3O_4 -MWNT nanoconjugate is shown in Figure 8(a). Impedance equivalent circuit used for fitting of the plot is shown in the inset of Figure 8(a). R1 represents the electrolyte resistance between working and reference electrodes in the equivalent circuit. Circuit also contains another resistance component R_2 which is the charge transfer resistance. A constant phase element(CPE) is also present in parallel to the charge transfer resistance. This CPE is introduced where non-ideal behaviour of the capacitance is required to be simulated. Another component is also introduced in the equivalent circuit called the Warburg element, W, in series with the charge transfer resistance. The Warburg element signifies the diffusion process that occurs at working electrode's surface.The plot between real and imaginary component of impedance and phase shift with change in frequency is shown in Figure 8(b-d). These plots show the changes of real and imaginary components of the impedance with change in frequency. It can be observed that the real and the imaginary components of the impedance are very high in very low frequency region. These values reduce to around 160 Ω for real component and around 13 Ω for the imaginary

component in the high frequency region. Similar behaviour is also observed for the phase shift with change in frequency from low to high.

The fitting of the nyquist plot was done using Zview software as per the equivalent circuit shown in the inset of Figure 8(a). The values calculated from the fitting of the curve as listed in Table 2. It can be observed from the Table 2 that the value for electrolyte resistance between working and reference electrode is 12.54 Ω, which is low. The value for charge transfer resistance was found to be 0.189 kΩ-cm^2. The values obtained from the fitting of the nyquist plot show that the Fe_3O_4-MWNT nanoconjugate has good electrochemical response and therefore can be used for electrochemical studies [36].

Table 2. Parameters calculated from fitting of the nyquist plot of Fe_3O_4-MWNT nanoconjugate.

WE	**Fe_3O_4 - MWNT**
R_1 (Ω)	12.54
R_2 (kΩ-cm^2)	0.189
CPE (S·s^n-cm^2)	3.36×10^{-4}
W (Ω-cm^2)	1117.8
n	0.147

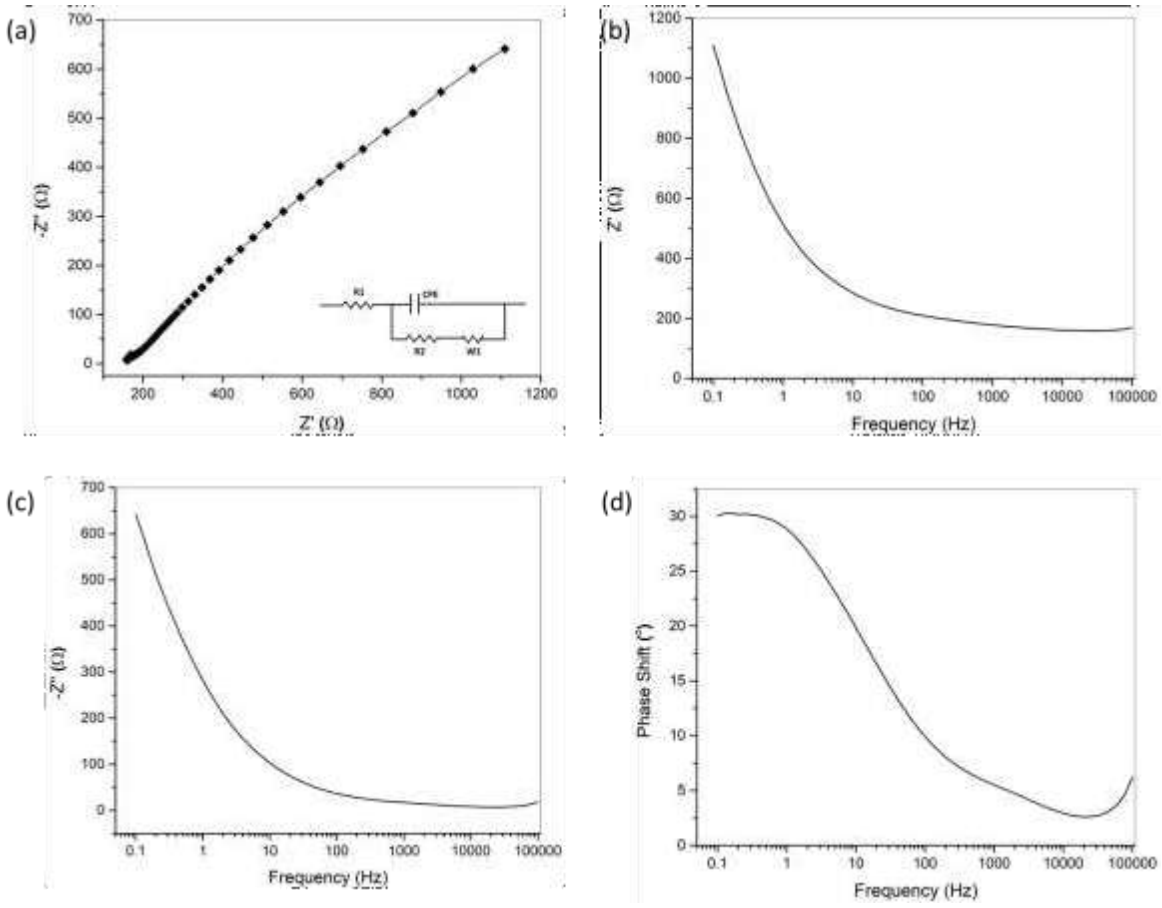

Figure 8: Electrochemical impedance spectroscopy of Fe_3O_4/MWNT nanoconjugate; (a) nyquist plot, (b) Z' vs frequency, (c) –Z'' vs frequency, and (d) phase shift vs frequency.

4. Conclusion

In this work, iron oxide nanoparticles (Fe_3O_4), and Fe_3O_4 – MWNT nano-conjugate successfully synthesized using the NANOCORPS^{TM} VX100 nanomaterial synthesis instrument. The synthesized nanoparticles and nano-conjugate has been successfully characterized using XRD, TEM, Raman spectroscopy, VSM and electrochemical impedance spectroscopy. The synthesis of nanoparticles and nano-conjugate using this instrument is single step and easy. It gives an advantage over other methods for synthesis of nano-conjugates which require use of different expensive chemicals and involve multiple steps. Using this instrument for synthesis of nanomaterials and nano-conjugates saves time and requires few chemicals. Therefore, this instrument is an inexpensive alternative over other synthesis methods and is capable of synthesizing and direct conjugation of a wide range of nanomaterials.

5. References

1. G. Modugno, C. Ménard-Moyon, M. Prato, and A. Bianco, "Carbon nanomaterials combined with metal nanoparticles for theranostic applications," *British Journal of Pharmacology*, vol. 172, pp. 975-991, 2015.
2. A. Eatemadi, H. Daraee, H. Karimkhanloo, M. Kouhi, N. Zarghami, A. Akbarzadeh, *et al.*, "Carbon nanotubes: properties, synthesis, purification, and medical applications," *Nanoscale Research Letters*, vol. 9, p. 393, 2014/08/13 2014.
3. J. Wallyn, N. Anton, and T. F. Vandamme, "Synthesis, Principles, and Properties of Magnetite Nanoparticles for In Vivo Imaging Applications-A Review," *Pharmaceutics*, vol. 11, p. 601, 2019.
4. W. Wu, Q. He, and C. Jiang, "Magnetic Iron Oxide Nanoparticles: Synthesis and Surface Functionalization Strategies," *Nanoscale Research Letters*, vol. 3, p. 397, 2008/10/02 2008.
5. M. Samadishadlou, M. Farshbaf, N. Annabi, T. Kavetskyy, R. Khalilov, S. Saghfi, *et al.*, "Magnetic carbon nanotubes: preparation, physical properties, and applications in biomedicine," *Artificial Cells, Nanomedicine, and Biotechnology*, vol. 46, pp. 1314-1330, 2018/10/03 2018.
6. J. Li, Y. Zhu, X. Wang, J. Zhang, Y. Ding, X. Zhang, *et al.*, "Joint effect of the tube sizes and Fe-filling process on microwave dielectric properties of carbon nanotubes," *Carbon*, vol. 119, pp. 386-393, 2017/08/01/ 2017.
7. F. S. Boi, Y. Hu, S. Wang, and Y. He, "Controlling high coercivities in cm-scale buckypapers with unusual stacking of vertically aligned and randomly entangled Fe-filled carbon nanotubes," *RSC Advances*, vol. 6, pp. 69226-69232, 2016.
8. D. Serrano-Ruiz, M. Laurenti, J. Ruiz-Cabello, E. López-Cabarcos, and J. Rubio-Retama, "Hybrid microparticles for drug delivery and magnetic resonance imaging," *J Biomed Mater Res B Appl Biomater*, vol. 101, pp. 498-505, May 2013.
9. K. Holmberg and A. Mathews, "Coatings tribology: a concept, critical aspects and future directions," *Thin Solid Films*, vol. 253, pp. 173-178, 1994/12/15/ 1994.
10. G.-L. Tian, J.-Q. Huang, J. Li, Q. Zhang, and F. Wei, "Enhanced growth of carbon nanotube bundles in a magnetically assisted fluidized bed chemical vapor deposition,"

Carbon, vol. 108, pp. 404-411, 2016/11/01/ 2016.

11. L. Zhang, Q.-Q. Ni, T. Natsuki, and Y. Fu, "Carbon nanotubes/magnetite hybrids prepared by a facile synthesis process and their magnetic properties," *Applied Surface Science*, vol. 255, pp. 8676-8681, 2009/07/30/ 2009.
12. Z. Liu, K. Chen, C. Davis, S. Sherlock, Q. Cao, X. Chen, *et al.*, "Drug delivery with carbon nanotubes for in vivo cancer treatment," *Cancer Res*, vol. 68, pp. 6652-60, Aug 15 2008.
13. R. Klingeler, S. Hampel, and B. Büchner, "Carbon nanotube based biomedical agents for heating, temperature sensoring and drug delivery," *Int J Hyperthermia*, vol. 24, pp. 496-505, Sep 2008.
14. S. Shen, J. Ren, X. Zhu, Z. Pang, X. Lu, C. Deng, *et al.*, "Monodisperse magnetites anchored onto carbon nanotubes: a platform for cell imaging, magnetic manipulation and enhanced photothermal treatment of tumors," *Journal of Materials Chemistry B*, vol. 1, pp. 1939-1946, 2013.
15. C. Chen, J. Hu, D. Shao, J. Li, and X. Wang, "Adsorption behavior of multiwall carbon nanotube/iron oxide magnetic composites for Ni(II) and Sr(II)," *Journal of Hazardous Materials*, vol. 164, pp. 923-928, 2009/05/30/ 2009.
16. C. Huiqun, Z. Meifang, and L. Yaogang, "Decoration of carbon nanotubes with iron oxide," *Journal of Solid State Chemistry*, vol. 179, pp. 1208-1213, 2006.
17. G. Sun, B. Dong, M. Cao, B. Wei, and C. Hu, "Hierarchical Dendrite-Like Magnetic Materials of Fe3O4, γ-Fe2O3, and Fe with High Performance of Microwave Absorption," *Chemistry of Materials*, vol. 23, pp. 1587-1593, 2011.
18. J. Wan, W. Cai, J. Feng, X. Meng, and E. Liu, "In situ decoration of carbon nanotubes with nearly monodisperse magnetite nanoparticles in liquid polyols," *Journal of Materials Chemistry*, vol. 17, p. 1188, 2007.
19. Y.-J. Lu, K.-C. Wei, C.-C. M. Ma, S.-Y. Yang, and J.-P. Chen, "Dual targeted delivery of doxorubicin to cancer cells using folate-conjugated magnetic multi-walled carbon nanotubes," *Colloids and Surfaces B: Biointerfaces*, vol. 89, pp. 1-9, 2012.
20. R. Rajarao, R. P. Jayanna, V. Sahajwalla, and B. R. Bhat, "GreenApproach to Decorate Multi-walled Carbon Nanotubes by Metal/Metal Oxide Nanoparticles," *Procedia Materials Science*, vol. 5, pp. 69-75, 2014.
21. J. Deng, X. Wen, and Q. Wang, "Solvothermal in situ synthesis of Fe3O4-multi-walled carbon nanotubes with enhanced heterogeneous Fenton-like activity," *Materials Research Bulletin*, vol. 47, pp. 3369-3376, 2012.
22. Y. Chen and H. Gu, "Microwave assisted fast fabrication of Fe3O4-MWCNTs nanocomposites and their application as MRI contrast agents," *Materials Letters*, vol. 67, pp. 49-51, 2012.
23. R. R. Shaoqing Song, Hongxiao Yang, Huade Liu and and A. Zhang, "Facile synthesis of Fe3O4/MWCNTs by spontaneous redox and their catalytic performance," *Nanotechnology*, vol. 21, 2010.
24. X. Zeng, L. Zhu, B. Yang, and R. Yu, "Necklace-like Fe3O4 nanoparticle beads on carbon nanotube threads for microwave absorption and supercapacitors,"

Materials & Design, vol. 189, p. 108517, 2020.

25. Thaar M. D. Alharbi, A. H. M. Al-Antaki, M. Moussa, W. D. Hutchison, and C. L. Raston, "Three-step-in-one synthesis of supercapacitor MWCNT superparamagnetic magnetite composite material under flow," *Nanoscale Advances,* vol. 1, pp. 3761-3770, 2019.
26. A. K. Mishra and S. Ramaprabhu, "Nano magnetite decorated multiwalled carbon nanotubes: a robust nanomaterial for enhanced carbon dioxide adsorption," *Energy Environ. Sci.,* vol. 4, pp. 889-895, 2011.
27. C. Wang, J. Yan, X. Cui, D. Cong, and H. Wang, "Preparation and characterization of magnetic hollow PMMA nanospheres via in situ emulsion polymerization," *Colloids and Surfaces A: Physicochemical and Engineering Aspects,* vol. 363, pp. 71-77, 2010.
28. A. Ruíz-Baltazar, R. Esparza, G. Rosas, and R. Pérez, "Effect of the Surfactant on the Growth and Oxidation of Iron Nanoparticles," *Journal of Nanomaterials,* vol. 2015, pp. 1-8, 2015.
29. S. Dutta, S. Sharma, A. Sharma, and R. K. Sharma, "Fabrication of Core-Shell-Structured Organic-Inorganic Hybrid Nanocatalyst for the Expedient Synthesis of Polysubstituted Oxazoles via Tandem Oxidative Cyclization Pathway," *ACS Omega,* vol. 2, pp. 2778-2791, Jun 30 2017.
30. B. Thapa, D. Diaz-Diestra, J. Beltran-Huarac, B. R. Weiner, and G. Morell, "Enhanced MRI T 2 Relaxivity in Contrast-Probed Anchor-Free PEGylated Iron Oxide Nanoparticles," *Nanoscale Res Lett,* vol. 12, p. 312, Dec 2017.
31. Y. M. Chen, C. A. Chen, Y. S. Huang, K. Y. Lee, and K. K. Tiong, "Characterization and enhanced field emission properties of IrO2-coated carbon nanotube bundle arrays," *Nanotechnology,* vol. 21, p. 035702, Jan 22 2010.
32. J. M. Feng and Y. J. Dai, "Water-assisted growth of graphene on carbon nanotubes by the chemical vapor deposition method," *Nanoscale,* vol. 5, pp. 4422-6, May 21 2013.
33. X. Zhang, J. Zhang, J. Quan, N. Wang, and Y. Zhu, "Surface-enhanced Raman scattering activities of carbon nanotubes decorated with silver nanoparticles," *Analyst,* vol. 141, pp. 5527-34, Oct 7 2016.
34. Y.-S. Li, J. S. Church, and A. L. Woodhead, "Infrared and Raman spectroscopic studies on iron oxide magnetic nano-particles and their surface modifications," *Journal of Magnetism and Magnetic Materials,* vol. 324, pp. 1543-1550, 2012.
35. J. Safari and S. Gandomi-Ravandi, "Fe3O4–CNTs nanocomposites: a novel and excellent catalyst in the synthesis of diarylpyrimidinones using grindstone chemistry," *RSC Adv.,* vol. 4, pp. 11486-11492, 2014.
36. M. Bagherzadeh, O. Mousavi, and Z. Shams Ghahfarokhi, "Fabrication and characterization of a Fe3O4/polyvinylpyrrolidone (Fe3O4/PVP) nanocomposite as a coating for carbon steel in saline media," *New Journal of Chemistry,* vol. 44, pp. 15148-15156, 2020.